Real time analysis of the RNAI-RNAII-Rop complex by surface plasmon resonance: from a decaying surface to a standard kinetic analysis.

Carmelo Di Primo

Real time analysis of the RNAI-RNAII-Rop complex by surface plasmon resonance: from a decaying surface to a standard kinetic analysis.

Short title: **Kinetic analysis of RNAI-RNAII-Rop by surface plasmon resonance.**

Carmelo Di Primo[1,2]

RNA loop-loop complexes are motifs that regulate biological functions in both prokaryotic and eukaryotic organisms. In *E. coli*, RNAI, an antisense RNA encoded by the ColE1 plasmid, regulates the plasmid replication by recognizing through loop-loop interactions RNAII, the RNA primer that binds to the plasmidic DNA to initiate the replication. Rop, a plasmid encoded homodimeric protein interacts with this transient RNAI-RNAII kissing complex. A surface plasmon resonance (SPR)-based biosensor was used to investigate this protein-nucleic acid ternary complex, at 5 °C, in experimental conditions such as the protein binds either to the loop-loop complex while it dissociates or to a saturated stable RNAI-RNAII surface. The results show that RNAI hairpin dissociates from the RNAII surface 110 times slower in the presence of Rop than in its absence. Rop binds to RNAI-RNAII with an on-rate of 3.6 10^6 $M^{-1}s^{-1}$ and an off-rate of 0.11 s^{-1}, resulting in a binding equilibrium constant equal to 31 nM. A Scatchard-plot analysis of the interaction monitored by SPR confirms a 1:1 complex of Rop and RNAI-RNAII as observed for non-natural Rop-loop-loop complexes.

Keywords: surface plasmon resonance; nucleic acids; RNA-protein interaction; kinetics

Received 26 july 2007; revised 5 september 2007; accepted 7 september 2007.

Abbreviations used. DIS, dimerization initiation site; HIV-1, human immunodeficiency virus type 1; SPR, surface plasmon resonance; RU, resonance unit.

[1]INSERM U869, Institut Européen de Chimie et Biologie, Pessac, F-33607, France; [2]Université Victor Segalen, Bordeaux, F-33076, France. Tel: 33 5 40 00 30 50, Fax: 33 5 40 00 30 04; E-mail: c.diprimo@iecb.u-bordeaux.fr.

INTRODUCTION.

RNA-RNA interactions formed between stem-loop structures are motifs that regulate biological functions in both prokaryotic and eukaryotic organisms (Brunel *et al*., 2002). The dimerization initiation site (DIS) of HIV-1, for instance, triggers the retroviral RNA dimerization through the formation of a transient kissing complex between two DIS elements (Ennifar *et al*., 2001; Muriaux *et al*., 1996; Paillart *et al*., 1996). A loop-loop complex might also regulate the RNA replication of the Hepatitis C virus (Song *et al*., 2006). Non natural loop-loop complexes were also identified through in vitro selection of RNA and DNA aptamers against viral RNA targets (Boiziau *et al*., 1999; Collin *et al*., 2000; Ducongé *et al*., 2000; Ducongé and Toulmé, 1999). Despiste a limited number of base pairs engaged between the loops, such hairpin pairs were shown to display higher specificity than linear sequences of similar affinity for their targets (Darfeuille *et al*., 2006). Non-canonical interactions are crucial and provide additionnal stability to these complexes (Beaurain *et al*., 2003; Chang and Tinoco, 1997; Ducongé *et al*., 2000; Lee and Crothers, 1998; Paillart *et al*., 1997). This is best illustrated with the Moloney murine leukemia virus that displays in its 5' end three stem-loops crucial for the dimerization of the viral RNA. The H3 stem-loops form a stable homodimeric kissing complex through two base pairs only (Kim and Tinoco, 2000; Li *et al*., 2006).

In prokaryotic organisms, RNA-RNA interactions through loop-loop recognition were also identified as key regulatory elements. In *E. coli*, in response to oxidative stress, the *fhla* mRNA folds as three adjacent stem-loop structures and is engaged in two loop-loop interactions with OxyS, a small untranslated RNA that displays two adjacent hairpins (Altuvia and Wagner, 2000; Altuvia *et al*., 1998; Argaman and Altuvia, 2000). Multiple loop-loop interactions between adjacent hairpins were also shown to control the translation of a crucial mRNA for the expression of virulence genes in *S. aureus* (Boisset *et al*., 2007; Geisinger *et al*., 2006). In this Gram-positive pathogen, RNAIII is the intracellular effector for the quorum-sensing system that regulates the synthesis of a major transcription factor, Rot, by blocking the translation of its mRNA (Boisset *et al*., 2007; Geisinger *et al*., 2006).

In *E. coli*, loop-loop interactions between two plasmid-encoded RNA transcripts, RNAI and RNAII, regulate the ColE1 plasmid replication (Eguchi and Tomizawa, 1990; Eguchi and Tomizawa, 1991). RNAI, an antisense RNA that

folds as three adjacent hairpins, recognizes the RNAII primer through loop-loop interactions preventing the formation of the RNA-DNA hydrid required to initiate the replication. Rop, a homodimeric protein encoded by the plasmid, plays a key role by stabilizing this transient complex (Eguchi and Tomizawa, 1990). Rop can also interact with non natural kissing complexes identified either by rationnal (Comolli *et al*., 1998) or combinatorial (Darfeuille *et al*., 2001; Di Primo and Lebars, 2007) approaches.

Surface plasmon resonance (SPR)-based biosensors that follow interactions in real time between an immobilized ligand and an injected analyte can be performed in a wide range of temperature (4 °C to 40 °C) for determining the binding equilibrium constant, the rates and the stoichiometry of a reaction (Fivash *et al*., 1998; Morton and Myszka, 1998; Van Regenmortel, 2001). SPR was successfully used to characterize interactions with small molecules to whole organisms (for review see (Rich and Myszka, 2006)), and to probe molecular recognition between proteins and nucleic acids (Di Primo and Lebars, 2007; Fisher *et al*., 2006; Law *et al*., 2006). Since their discovery, Rop-RNA kissing complexes have been investigated by biochemical methods such as mutagenesis experiments (Predki *et al*., 1995) and enzymatic footprintings (Eguchi and Tomizawa, 1990; Eguchi and Tomizawa, 1991). NMR (Comolli *et al*., 1998), fluorescence (Rist and Marino, 2001) and UV-absorption spectroscopies (Comolli *et al*., 1998) were used to probe in solution the interaction between Rop and natural or artificial loop-loop complexes. Three works used SPR-based instruments to analyze Rop binding to RNA kissing complexes. In the first one, the protein was used only as a molecular probe to demonstrate that apical-loop-internal-loop RNA-RNA complexes adopted an overall conformation different from that of RNA loop-loop complexes (Aldaz-Carroll *et al*., 2002). In the second one, SPR was used to assess the binding equilibrium constant between Rop and RNAIinv-RNAIIinv, an RNA hairpin pair that displayed inverted loops compared with those of the natural complex (Christ and Winter, 2003). This loop inversion resulted in a much higher stability of the former over the latter that enabled its solution structure determination (Lee and Crothers, 1998). More recently Rop binding to artificial loop-loop complexes was used to demonstrate that nucleic acids and proteins behave similarly with respect to the refractive index increment they induce upon binding to a surface (Di Primo and Lebars, 2007). However none of these studies addressed kinetic issues and recognition between Rop and RNAI-RNAII, with wild-type loops, has never been analyzed by SPR likely because the loop-loop complex is very unstable at room temperature.

In an SPR experiment, depending on how molecules interact, complexes of more than two partners can generate data really complicated to analyze. In an assay involving for instance three molecules, a ligand is immobilized on the sensor surface usually for capturing a first analyte that will recognize a second one. During binding of the latter, the former dissociates from the surface. In a classical capturing experiment the first immobilized partner is used only for capturing the target which is one partner of the complex of interest. In some cases the capturing ligand can be designed to make negligible the dissociation of the captured target from the surface but when this cannot be achieved two reactions contribute simultaneously to the recorded sensorgrams. Joss et al. demonstrated that kinetic rate constants could be determined on a decaying surface designed to monitor a Fab-antigen interaction (Joss *et al*., 1998). In this example, the dissociation rate for binding the injected antigen to the immobilized capturing ligand was similar in the presence or in the absence of the third partner.

If RNAII is immobilized for capturing RNAI and Rop is injected to form the RNA-RNA-protein complex, RNAI dissociates from RNAII during binding of the protein, as expected. However RNAII is not only a capturing ligand but also directly involved in the nucleic acid-protein ternary complex (Eguchi and Tomizawa, 1991). In addition Rop was shown to decrease the dissociation rate of the loop-loop complex (Eguchi and Tomizawa, 1991). In other words the dissociation rate of RNAI-RNAII is not similar in the presence or in the absence of the protein Rop, complicating even more the data analysis.

In this work, using simple experimental conditions, an SPR experiment that gives crucial but limited informations is converted into an standard kinetic assay that permits for Rop binding to RNAI-RNAII to determine the binding equilibrium constant, in steady-state conditions or by the ratio of the rate constants, and the stoichiometry of the reaction. In agreement with previous works, the results obtained by SPR analysis show that Rop binding to RNAI-RNAII occurs in the low nanomolar range with a stoichiometry of 1:1 and that binding of the protein decreases the dissocation rate of the loop-loop complex.

MATERIALS AND METHODS.

Oligonucleotides and protein. RNAI and RNAII, labeled with a 3' biotin-TEG(Figure 1a) were synthesized on a Expedite 8908 synthesizer and purified by electrophoresis on denaturing polyacrylamide gels. Pure samples were desalted using G-25 spin columns prepared in 2 ml syringes. The protein Rop was purified as described previously (Di Primo and Lebars, 2007). Briefly, Rop was expressed in *E. coli* as a fusion protein with a 6-histidine tag and purified on nickel HisTrap FF Crude 5 ml columns (Amersham Biosciences). The tag was then removed by an overnight incubation of Rop with the tobacco etch virus protease at 25 °C. The samples were further purified on HiTrap QFFQ-sepharose anion-exchange columns (Amersham Biosciences). Pure samples were assayed at 280 nm using an extinction coefficient of 0.24 cm^2/mg and stored at –80 °C in 5 μl aliquots.

Surface plasmon resonance experiments. SPR experiments were performed on a BIAcore^{TM} 3000 apparatus (Biacore, GE Healthcare, Uppsala, Sweden). Fourty-seven RU of biotinylated RNAII was immobilized on a streptavidin coated SA sensorchip (Biacore) prepared according to the manufacturer's instructions. One flowcell left blank was used as reference. Binding experiments

performed in duplicate were carried out at 5 °C in 10 mM sodium phosphate buffer, pH 7.2 at 21 °C, containing 140 mM potassium chloride, 5 mM magnesium chloride, 1 mM DTT and 0.005% surfactant P20 (running buffer). RNAI and Rop were prepared in the running buffer and injected at 20 μl/min across the sensor surface. The regeneration of the RNAII-coated surface was achieved with a 1-minute pulse of a 20 mM EDTA solution followed by a 1-minute pulse of running buffer.

The sensorgrams, recorded at 5 Hz data collection rate, were double-referenced using BiaEval 4.1 software (Biacore) to remove instrument noises and the buffer contribution to the signals (Myszka, 1999). They were also normalized in x- and y-axis to account for small variations of the baseline and the start injection point. The sensorgrams were of good enough quality that there was no need prior to data fitting to discard points either at the beginning or at the end of the injection of the samples. Spikes still present after this normalization process had absolutely no influence on the kinetic parameters determined by direct fitting of the sensorgrams.

Kinetic titration of RNAI-RNAII. Kinetic titration experiments were performed to determine the rate constants, k_{-1} and k_{+1}, and the binding equilibrium constant, Kd_{kis}, for the RNAI-RNAII complex formation, as described previously (Karlsson *et al*., 2006). This method provides a way to determine the kinetic parameters within one single binding cycle and without need of regeneration between each sample injection. It is faster and as reliable as the classical method which consists in performing several kinetic cycles at increasing concentration of the injected analyte, with a regeneration step between each cycle. Three concentrations of RNAI prepared in the running buffer were injected sequentially in order of increasing concentration over both the RNAII immobilized ligand and the blank surfaces. The association and dissociation rate constants, k_{+1} and k_{-1}, respectively, were determined from direct curve fitting of the sensorgrams obtained by this method with BiaEval 4.1 (Biacore), assuming a simple reversible mechanism according to Equations 1 and 2, for the association and the dissociation phases, respectively:

$$\frac{dRU}{dt} = k_{+1}[RNAI]RU_{\max 1} - (k_{+1}[RNAI] + k_{-1})RU \qquad (1)$$

$$\frac{dRU}{dt} = -k_{-1}RU_{t0}.e^{-k_{-1}(t-t_0)} \qquad (2)$$

where RU is the signal response, RU_{max1} the maximum response level, RU_{t0} the response at the beginning of the dissociation phase, and [RNAI] the molar concentration of the injected RNAI molecule. The binding equilibrium constant, Kd_{kis}, was calculated as k_{-1}/k_{+1}. The model to fit globally such sensorgrams was not available in the BiaEval software but it was easily created writing the formulas for a kinetic titration data set of three analyte injections, as described previously (Karlsson *et al*., 2006).

Kinetics of Rop binding to RNAI-RNAII. Binding of Rop to the RNA-RNA complex was analyzed by the classical method which consists in injecting several analyte concentrations over the target surface and regenerating it between binding cycles. The kissing complex was first formed by injected RNAI at saturating concentration (1.5 μM) over the RNAII surface. Rop was then injected at increasing concentration over the generated RNAI-RNAII surface, in the absence or in the presence of RNAI. The sensorgrams were fitted globally using BiaEval 4.1 assuming, in addition to the RNAI-RNAII binding reaction, one reaction that describes Rop binding to the newly formed loop-loop complex, including a mass transport step, according to Equations 3 and 4 for the association and the dissociation phases, respectively:

$$\frac{dRU}{dt} = k_n[Rop] - \frac{k_n k_{-2}}{k_{+2}(RU_{\max 2} - RU)}RU \qquad (3)$$

$$\frac{dRU}{dt} = -k_{-2}RU_{t0}.e^{-k_{-2}(t-t_0)} \qquad (4)$$

where k_n is the rate constant for mass transport, k_{+2} and k_{-2} the association and dissociation rate constants, respectively, RU the signal response, RU_{max2} the maximum level response upon Rop binding to the loop-loop surface, RU_{t0} the response at the beginning of the dissociation phase and [Rop] the molar concentration of the injected protein.

The binding equilibrium constant, Kd_{Rop}, was determined either as k_{-2}/k_{+2} or by using a Scatchard-plot of $RU_{eq}/[Rop]$ as a function of RU_{eq}, where RU_{eq} is the response measured in the steady-state region (plateau) of the sensorgrams and [Rop] is the corresponding protein concentration. The stoichiometry of the reaction was determined from such plots using the expected maximum response upon binding of Rop, $(RU_{exp})_{max2}$, calculated according to Equation 5:

$$(RUexp)max2 = RURNAI * \frac{MWRop}{MWRNAI} \qquad (5)$$

where RU_{RNAI} is the amount of RNAI bound to the RNAII surface, MW_{rop} and MW_{RNAI} the molecular weights of Rop and RNAI, respectively.

RESULTS.

Figure 1b describes all the reactions that can give rise to the recorded sensorgrams. In addition to the main reactions that describe the formation of the RNAI-RNAII followed by Rop binding to this complex, with corresponding rate constants k_{-1} and k_{+1}, and k_{-2} and k_{+2}, respectively, three other reactions may have to be considered. Two reactions with rate constants k_m and k_n may account for mass-transport effects either when RNAI or Rop are injected, respectively. These reactions describe the transport of RNAI or Rop from bulk solution to the reaction surface. The mass transport constant depends only on flow cell dimensions and bulk flow rate as well as on the diffusion properties of the analyte in the sample solution (Karlsson *et al*., 1994; Sjölander and

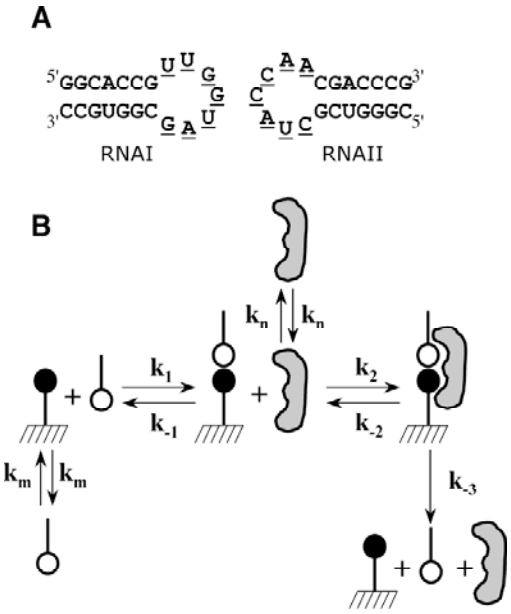

Figure 1. RNA molecules and reaction-scheme for the interaction of Rop with the loop-loop complex. A) Sequence and secondary structure of RNAI and RNAII 3'-biotinylated. The bases susceptible to base pair are underlined. B) Reaction-scheme of Rop binding to RNAI-RNAII. Rop is depicted in grey, white and black circles represent RNAI and RNAII loops, respectively. RNAII was immobilized on SA sensorchips (dashed lines).

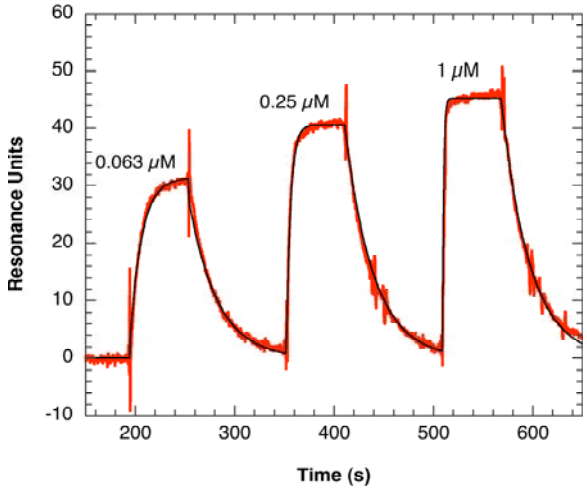

Figure 2. Kinetic analysis of RNAI-RNAII complex formation. Kinetic parameters were determined by the kinetic titration method. RNAI (0.063 μM, 0.25 μM and 1 μM) prepared in the running buffer was injected at 20μl/min for 1 min across the RNAII surface. The red curve represents the experimental data and the black one the fit of the sensorgram to a kinetic titration data set of three analyte injections.

Urbaniczky, 1991). These rates are then expected to be the same for mass transport to and from the surface. If transport is much faster than association of analyte with the immobilized ligand, the binding will be determined by the interaction constants (k_{-1}, k_{+1}, k_{-2} and k_{+2}). On the contrary no kinetics will be obtained if it is much slower. Between these extremes both mass transport and interaction kinetics will contribute to the observed binding. A third reaction with rate constant k_{-3} corresponds to the dissociation of the loop-loop complex in the presence of the protein.

In a first experiment, a kinetic titration assay was carried out to determine k_{+1} and k_{-1}. The sensorgrams were recorded at 5 °C since the binding kinetics for RNAI-RNAII complex formation were too fast to be measured at room temperature (data not shown). Three RNAI samples were injected sequentially as shown in Figure 2. The sensorgrams were fitted to a kinetic titration 1:1 interaction model as described in Materials and Methods. Good fits were obtained without need to include a mass transport step. k_{+1} and k_{-1} are equal to 8.2 10^5 ± 0.3 10^5 M^{-1} s^{-1} and 351 10^{-4} ± 1 10^{-4} s^{-1}, respectively, resulting in an affinity, Kd_{kis}, of 43 ± 2 nM (Table1).

To analyze Rop binding to RNAI-RNAII, a loop-loop surface was first prepared by injecting RNAI at saturating concentration, 1.5 μM, over the RNAII immobilized ligand. Rop was then injected at increasing concentration (0 to 10 μM) between 512 and 572 s, as shown in Figure 3. Sensorgrams apparently similar to those recorded on a decaying surface are observed clearly showing that the hairpin pair dissociates while the protein binds. However the fit of these sensorgrams to a simple 1:1 interaction model for binding the protein to the nucleic acid complex on a decaying surface as described previously (Joss *et al.*, 1998) is absolutely not consistent with the experimental data (Figure 3). In a classical capturing assay on a decaying surface as that described previously (Joss *et al.*, 1998), the dissociation rate for binding the captured ligand was similar in the absence or in the presence of the third partner which only recognized the captured one (the second partner). In other words, the surface decayed with one rate only even when the third partner bound. Rop binds only to the kissing complex, not to the hairpins alone (data not shown) and the dissociation rate of RNAI-RNAII is clearly faster in the absence of Rop than in its presence. When the protein is injected between 512 and 572 s (below 10 μM), the surface decays with two rates and basically with one when the injection is stopped since the protein dissociates more rapidly from RNAI-RNAII than this complex dissociates in the presence of the protein (compare dissociations after 572 s and between 512 and 572 s at 10 μM of Rop). Using the commercially available BiaEval software and globally fitting the data, we could not account for a surface that decayed with two rates when Rop was injected. Nevertheless, in such experimental conditions one crucial parameter can be determined that is the dissociation rate of the loop-loop complex in the presence of the protein, k_{-3}. This rate can be simply determined by fitting to a single decaying exponential function (not shown) the sensorgram obtained at saturating concentration of protein (10 μM) between 512 and 572 s only, during the association phase of the protein binding to the loop-loop complex. k_{-3} is equal to 3.2 10^{-4} ± 0.3 10^{-4} s^{-1}. Dissociation of RNAI-RNAII at 5°C is 110 times slower in the presence of the protein than in its absence (Table 1).

The question arises now how to determine the binding equilibrium constant, the rates and the stoichiometry of a

Table 1. Equilibrium and rate constants for RNAI-RNAII complex formation and for Rop binding to RNAI-RNAII.

Complex	k_{+1} $\times 10^{5}M^{-1}s^{-1}$	k_{-1} $\times 10^{-4}s^{-1}$	Kd_{kiss} nM	k_{-3} $\times 10^{-4}s^{-1}$	k_{+2} $\times 10^{6}M^{-1}s^{-1}$	k_{-2} $\times 10^{-2}s^{-1}$	Kd_{Rop} nM
RNAI-RNAII	8.2 ± 0.3	351 ± 1	43 ± 2	3.2 ± 0.3			
RNAI-RNAII-Rop							28 ± 1[a]
					3.6 ± 0.4[b]	11 ± 3[b]	31 ± 4[c]
					3.2 ± 0.2[d]	9 ± 1[e]	

[a]determined by Scatchard-plot analysis.
[b]determined by global fitting analysis of the sensorgrams shown in Figure 5a.
[c]calculated as k_{-2}/k_{+2}.
[d]k_{+2} was calculated as k_{-2}/Kd_{Rop}, where Kd_{Rop} was determined by Scatchard-plot analysis and k_{-2} by global fitting analysis of the dissociation phases shown in Figure 5b.
[e]determined by global fitting analysis of the dissociation phases shown in Figure 5b.

reaction between a protein and a bimolecular complex the stability of which varies depending on its binding status with the third partner. In fact, simple experimental conditions can be used to convert a set of sensorgrams that cannot be analyzed with the software provided by the manufacturer in perfectly informative data for determining these parameters. As observed previously (Figure 3), when RNAI is injected at saturating concentration across the RNAII surface, the sensorgram reaches instantenously a plateau. As long as RNAI is present in the injected flow, a new baseline is actually set for the sensorgrams. Then if the protein is injected at increasing concentration in the presence of RNAI at constant concentration, more classical sensorgrams are obtained even if the dissociation phases reflect obviously more than one dissociation reaction. Sensorgrams recorded in these new conditions are reported in Figure 4a. Binding of Rop is characterized by a well defined saturation level of the RNAI-RNAII surface. This will enable to determine the binding equilibrium constant, Kd_{rop}, not only kinetically but also by a Scatchard-plot analysis, and the stoichiometry of the reaction. This is will be usefull to compare and to validate the equilibrium constant determined kinetically with that obtained in steady-state conditions.

A Scatchard-plot of Rop binding to RNAI-RNAII is shown in Figure 4b. The plotted RU_{eq} values as a function of Rop concentration, [Rop], correspond to the RU values measured in the flat region of the sensorgrams (averaged value of a 10 s portion of the curve before the end of the injection, t = 549 s) minus the RU value when no protein was injected. The slope of the graph gives a binding equilibrium constant, Kd_{rop}, equal to 28 ± 1 nM (Table 1). The expected maximum response, $(RU_{exp})_{max2}$, upon binding of the protein to the loop-loop complex was used to determine the stoichiometry of the reaction. $(RU_{exp})_{max2}$ was calculated from the molecular weights of RNAI (6759 g/mole) and Rop (14844 g/mol), and the amount of RNAI bound to RNAII (47 RU), as described in Materials and Methods, without any corrective factor that may account for differences in refractive index increments between proteins and nucleic acids upon binding to a surface. Recently, by investigating complexes of known stoichiometry, we showed that proteins and nucleic acids behave similarly regarding refractive index increments changes (Di Primo and Lebars, 2007), in agreement with other studies (Tumolo *et al.*, 2004; ; Fisher *et al.*, 2006). The intersection of the Scatchard-plot with the $RU_{eq}/(RU_{exp})_{max}$ axis demonstrates that Rop recognizes the RNAI-RNAII complex with a 1:1 stoichiometry.

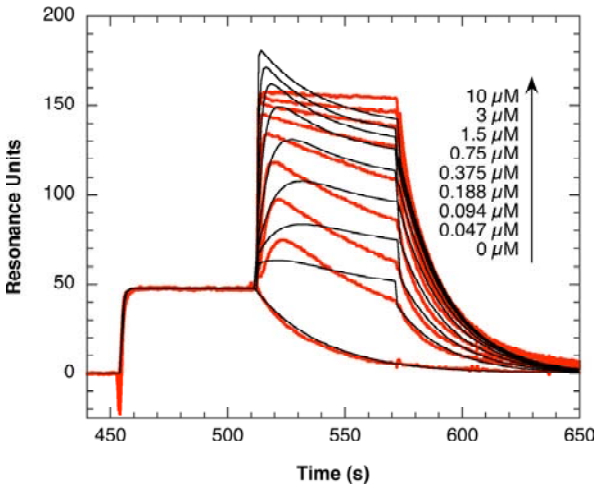

Figure 3. Kinetic analysis of Rop binding to an RNAI-RNAII decaying surface. A RNAI-RNAII surface was prepared by injecting RNAI at saturating concentration (1.5 μM) at 20 μl/min for 1 min across the RNAII surface. The "co-inject" command of the instrument was used to inject Rop immediately after the RNAI injection for 1 min at increasing concentrations as indicated by the arrow. The sensorgrams were globally fitted to a model that assumes binding of Rop (between 512 and 572 s) while RNAI-RNAII is dissociating. The red curves represent the experimental data and those in black the fit.

The recorded sensorgrams were then analyzed kinetically by global fitting to determine the rate contants, k_{+2} and k_{-2}, and the dissociation equilibrium constant, Kd_{Rop}, calculated as k_{-2}/k_{+2}. Two reactions were simultaneously considered. The first one corresponded to the RNAI-RNAII complex formation and the second one to the binding of Rop to this nucleic acid complex (Figure 1). To fit the sensorgrams, appropriate start- and stop-injection times were chosen for each reaction: 459 s and 549 s for the loop-loop interaction, respectively, and 504 s and 549 s for Rop interacting with RNAI-RNAII, respectively. The k_{+1} and k_{-1}values deduced from the kinetic titration experiment performed in the

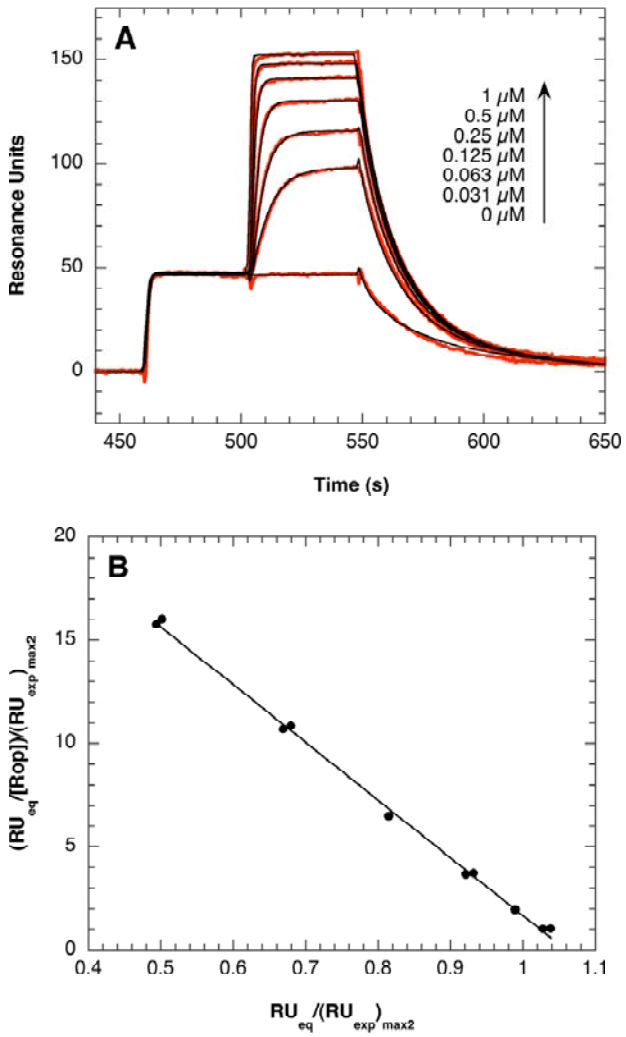

Figure 4. Kinetic and Scatchard analysis of Rop binding to RNAI-RNAII. A) Binding of Rop to RNAI-RNAII. A loop-loop surface was prepared by injecting RNAI at 20 μl/min for 45 s at saturating concentration (1.5 μM) across the RNAII surface. Rop was then injected at the same flow rate for 45 s at increasing concentration as indicated by the arrow, in the presence of RNAI at 1.5 μM to avoid the kissing complex dissociation while the protein was binding. The sensorgrams were globally fitted assuming simultaneously two reactions, one corresponding to the RNAI-RNAII complex formation with an association phase between 459 and 549 s, and one corresponding to the protein-RNA-RNA complex formation, including a mass transport step, with an association phase between 504 and 549 s. To fit the data k_{+1} and k_{-1} determined from the kinetic titration assays were used and left constant. The red curves represent the experimental data and those in black the fit. B) Scatchard-plot of Rop binding to RNA-RNAII. RU_{eq} is the averaged RU value measured during 10 s at the end of the association phase of the protein. $(RU_{exp})_{max2}$ is the expected maximum response upon binding of the protein to the kissing complex. $(RU_{exp})_{max2}$ was calculated as described in Materials and Methods assuming molecular weights for RNAI and Rop of 6759 g/mol and 14844 g/mol, respectively, and 47 RU of bound RNAI to the RNAII surface.

absence of Rop (Figure 2) were used and left constant as well as the concentration of the injected RNAI hairpin (1.5 μM). Best fit of the data for Rop binding was obtained assuming a 1:1 interaction model including a mass transport step. Increasing the flow rate of the sensorgrams to the highest value, 100 μl/min, had no effect on the shape of the

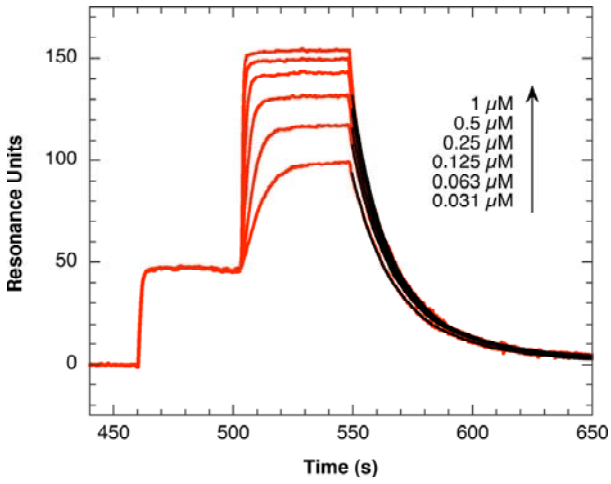

Figure 5. Dissociation phases analysis of the Rop-RNAI-RNAII complex. Experimental conditions are those described in Figure 4a. The observed dissociation phases were fitted to the sum of two decaying exponential functions. Only k_{-2}, the off-rate for Rop binding to the kissing complex, was assessed. k_{-1} determined by the titration assay was left constant. k_{+2}, the on-rate for Rop binding was calculated as k_{-2}/Kd_{Rop} using k_{-2} from this analysis and Kd_{Rop} from the Scatchard-plot analysis. The red curves represent the experimental data and those in black the fit.

curve obtained when Rop was injected at the lowest concentration, 31 nM, (data not shown), suggesting that Rop bound very quickly compared with the arrival rate of the analyte from the injection solution to the reaction region. This has been observed for other natural protein-nucleic acid complexes (Fisher *et al.*, 2006; Law *et al.*, 2006). Data analysis reveals that Rop binds to RNAI-RNAII with an association rate constant, k_{+2}, of 3.6 $10^6 \pm$ 0.4 10^6 M^{-1} s^{-1} and a dissociation rate constant, k_{-2}, of 0.11 ± 0.03 s^{-1}. This results in an affinity, Kd_{Rop}, of 31 ± 4 nM (Table 1). This value agrees very well with that determined by Scatchard-plot analysis (28 ± 1 nM) obtained by nature without knowing the rate constants k_{+1}, k_{-1}, k_{+2} and k_{-2}. This validates not only the thermodynamic parameters for Rop binding but also those found for the RNAI-RNAII complex formation since k_{-1} and k_{+1}, determined by the kinetic titration method, were used to assess k_{+2} and k_{-2} in the global fitting analysis.

To validate even more the binding parameters for the interaction of Rop with RNAI-RNAII, k_{+2} was determined by analyzing the dissociation phases and using Kd_{Rop} determined by Scatchard-plot analysis. The observed dissociation phases (Figure 5) describe mainly two fast reactions: the RNAI-RNAII and Rop-loop-loop complex dissociations, with off-rate contants k_{-1} and k_{-2}, respectively. In such conditions, the extremely slow dissociation of the RNAI-RNAII complex in the presence of Rop (k_{-3} = 3.2 10^{-4} s^{-1}) cannot be observed. The dissociation phases of the sensorgrams were fitted to the sum of two decaying exponential functions with k_{-1}, deduced from the titration experiment (Figure 2), left constant. k_{-2} is equal to 0.09 s^{-1}, on average, and k_{+2}, calcultated as k_{-2}/Kd_{Rop} is equal to 3.2 10^6 ± 0.2 10^6 M^{-1} s^{-1} (Table1). This on-rate value agrees is consistent with that obtained by direct fitting of the entire sensorgrams (3.6 10^6 M^{-1} s^{-1}).

DISCUSSION.

Rop binding to RNAI-RNAII plays a key role in *E. coli* and regulates the ColE1 plasmid replication by stabilizing a transient loop-loop complex formed between these two structured RNAs. To the best of our knowledge, Rop is a unique case of a protein recognizing such three-dimensional RNA motif by establishing contacts with both RNA hairpins. Rop binding to RNAI-RNAII is an interesting case to investigate by an SPR-based biosensor. In contrast to a classical capturing assay, the immobilized ligand, RNAII, is not just a capturing ligand but also one partner of the interaction (Eguchi and Tomizawa, 1991). Since Rop stabilizes the loop-loop complex, the sensorgrams are expected to be more complicated to analyze than those recorded during a classical capturing assay on a decaying surface.

To determine the binding parameters for the reaction of Rop with RNAI-RNAII, those for the loop-loop complex formation were determined first. Recognition between RNAI and RNAII occurs with an affinity of 43 nM, at 5 °C. Rapid dissociation of the complex (0.035 s^{-1}) is compensated by rapid association (8.2 10^5 M^{-1} s^{-1}). The thermodynamics of this complex has been analyzed previously by thermal denaturation monitored by UV-spectroscopy, in very close buffer conditions, in particular at the same magnesium concentration, 5 mM (Gregorian and Crothers, 1995). This cation was shown to strongly influence the stability of loop-loop complexes (Ducongé *et al.*, 2000; Gregorian and Crothers, 1995). Direct binding of two ions at specific sites results in an increased thermodynamic stability of such motifs. By analyzing the transition curves corresponding to the melting of the bimolecular complexes, an enthalpy of formation of RNAI-RNAII, ΔH_f, equal to –38 kcal/mol, on average, was obtained. Knowing the melting temperature of the complex (Tm = 40 °C) and the total strand concentration (2 μM), the free energy of complex formation, ΔG_f, can be determined. ΔG_f is equal to –10.4 ± 0.5 kcal/mol at 25 °C. Deduced from the SPR assay, ΔG_f is equal to –10.1 kcal/mol at 25 °C. The results obtained either in solution or at the interface between the sensorchip surface and the injection solution agree well.

Binding kinetics of the RNAI-RNAII complex formation were also analyzed, at 25 °C, by gel electrophoresis with radiolabeled hairpins, in a buffer containing 10 mM of magnesium ions (Eguchi and Tomizawa, 1990; Eguchi and Tomizawa, 1991). A lower complex stability was observed (ΔG_f = -9.1 kcal/mol at 25°C) despite a magnesium concentration twice higher. Considering that $\Delta\Delta G_f$ is equal to –1.1 kcal/mol upon increasing the magnesium concentration from 5 to 10 mM (Gregorian and Crothers, 1995), there is a discrepancy of about 2.3 kcal/mol between the results obtained by gel electrophoresis and those from UV-monitored or SPR experiments. By lack of other explanations, we are tempted to believe that this discrepancy is simply due to the fact that in the gel electrophoresis study, the equilibrium constant was assessed by estimating by partial digestion by RNAase A the relative amounts of free RNAII allowed to interact with RNAI. Kd_{kis} was not determined by thermodynamic or real time analysis, supposely more accurate methods for determining equilibrium constants, as being more direct.

Stoichiometry is crucial to understand function. Since the measured signal is caused by mass changes at the sensor chip surface, by simply comparing the expected maximum response with the observed one, upon binding of a molecule to the surface, SPR-based optical sensors provide an easy way to detect how many molecules interact together. A 1:1 complex of Rop and RNAI-RNAII was found by SPR analysis, in good agreement with a previous work that analyzed Rop binding to this complex by electrophoretic mobility shift assays in polyacrylamide gels (Eguchi and Tomizawa, 1990). Artificial Rop-loop-loop complexes investigated by NMR spectroscopy revealed that molecular recognition between this homodimeric protein and these RNA hairpins also occurred with a 1:1 stoichiometry (Comolli *et al.*, 1998; Di Primo and Lebars, 2007) indicating that Rop tolerates three-dimensional motifs that share common structural features. Previous work has shown that Rop is structure specific rather than sequence specific (Eguchi and Tomizawa, 1990).

Binding of Rop to a decaying RNAI-RNAII surface shows that RNAI dissociates from the RNAII surface 110 times slower at 5 °C in the presence of the protein than it its absence. This result is consistent with a previous work that showed that dissociation of RNAI-RNAII, measured at 25°C, was 267 times faster in the absence of Rop than it its presence (Eguchi and Tomizawa, 1990). Binding of Rop to RNAI-RNAII either with natural or inverted loop has been reported previously. A binding equilibrium constant, Kd_{Rop}, of 200 nM was found at 25 °C when the interaction was analyzed by gel electrophoresis with radiolabeled hairpins displaying natural loops (Eguchi and Tomizawa, 1990; Eguchi and Tomizawa, 1991). Analyzing binding to hairpin pairs with inverted loops either by SPR at 4 °C (Christ and Winter, 2003) or by fluorescence spectrocopy at 25 °C (Rist and Marino, 2001) led to Kd_{Rop} equal to 8 nM and 60 ± 24 nM, respectively. These results cannot be rigorously compared as they were obtained at different temperatures and with hairpins that differ in their 5' to 3' loop orientation. However, there is a clear trend and our results agree with that: molecular recognition between Rop and RNAI-RNAII occurs with an affinity in the low nanomolar range, at 5 °C. Our work is the first one that gives rate constants for this reaction. The protein dissociates rapidly from the loop-loop complex but binds also rapidly. This is expected to be crucial for efficient regulation of the ColE1 plasmid replication by rapid turnover of the protein-nucleic acid complex.

In a work published recently, binding of Rop to artificial loop-loop complexes was investigated by SPR (Di Primo and Lebars, 2007). In particular, Rop binding to a hairpin pair formed between truncated versions of the TAR RNA element of HIV-1 and its RNA aptamer was analyzed at 5 °C, in medium conditions not significantly different from those used in the present work. A binding equilibrium constant, Kd_{Rop}, of 3.6 μM was obtained, a value 129 times higher than for interacting with RNAI-RNAII. Although Rop recognizes a structure and not a sequence, the TAR-RNA aptamer complex and the natural one, RNAI-RNAII,

are clearly not equivalent regarding Rop recognition. These two complexes mainly differ by the size of the loops potentially engaged in Watson-Crick interactions, six and seven nucleotides for the former and the latter, respectively. The three-dimensional structure of several loop-loop complexes recognizing Rop were solved (Chang and Tinoco, 1994; Lee and Crothers, 1998) or modeled (Beaurain *et al*., 2003). The three-dimensional structure of the protein is known as well (Banner *et al*., 1983; Eberle *et al*., 1991; Jang *et al*., 2006) but that of protein-RNA-RNA ternary complexes is not yet established. Using these results, NMR data on another artificial complex between TAR and TAR* (Chang and Tinoco, 1997), a rationnally designed TAR ligand, mutagenesis (Predki *et al*., 1995) and ribonuclease cleavage data for the ColE1 kissing complex (Eguchi and Tomizawa, 1990; Eguchi and Tomizawa, 1991), a model of the binding of Rop to the TAR-TAR* complex was proposed (Comolli *et al*., 1998). This model suggests major contacts between the protein and the minor groove of the bimolecular loop-loop helix and minor contacts with the stem helices. The size of the bimolecular helix is then expected to be critical for optimizing the interaction between the protein and the RNA-RNA complex.

In conclusion our results show that Rop binding to RNAI-RNAII, the stability of which drastically increases in the presence of the protein, can be investigated by SPR experiments. Sensorgrams that gave limited informations, recorded first on a decaying surface, were converted into more classical curves that enabled for Rop binding to the ColE1 kissing complex to determine the rates, the binding equilibrium constant and the stoichiometry of the reaction.

ACKNOWLEDGMENTS.

This work was supported by the Institut National de la Santé et de la Recherche Médicale and the Institut Européen de Chimie et Biologie. We thank Thierry Dakhli for purifying Rop, Nathalie Pierre for synthesizing the RNA molecules, Jean-Jacques Toulmé and Isabelle Lebars for critically reading the manuscript.

REFERENCES.

Aldaz-Carroll L, Tallet B, Dausse E, Yurchenko L, Toulmé JJ. 2002. Apical loop-internal loop interactions: a new RNA-RNA recognition motif identified through in vitro selection against RNA hairpins of the hepatitis C virus mRNA. *Biochemistry* **41**: 5883-93.

Altuvia S, Wagner EG. 2000. Switching on and off with RNA. *Proc Natl Acad Sci U S A* **97**: 9824-6.

Altuvia S, Zhang A, Argaman L, Tiwari A, Storz G. 1998. The Escherichia coli OxyS regulatory RNA represses fhlA translation by blocking ribosome binding. *Embo J* **17**: 6069-75.

Argaman L, Altuvia S. 2000. fhlA repression by OxyS RNA: kissing complex formation at two sites results in a stable antisense-target RNA complex. *J Mol Biol* **300**: 1101-12.

Banner DW, Cesareni G, Tsernoglou D. 1983. Crystallization of the ColE1 Rop protein. *J Mol Biol* **170**: 1059-60.

Beaurain F, Di Primo C, Toulmé JJ, Laguerre M. 2003. Molecular dynamics reveals the stabilizing role of loop closing residues in kissing interactions: comparison between TAR-TAR* and TAR-aptamer. *Nucleic Acids Res* **31**: 4275-84.

Boisset S, Geissmann T, Huntzinger E, Fechter P, Bendridi N, Possedko M, Chevalier C, Helfer AC, Benito Y, Jacquier A, Gaspin C, Vandenesch F, Romby P. 2007. Staphylococcus aureus RNAIII coordinately represses the synthesis of virulence factors and the transcription regulator Rot by an antisense mechanism. *Genes Dev* **21**: 1353-66.

Boiziau C, Dausse E, Yurchenko L, Toulmé JJ. 1999. DNA aptamers selected against the HIV-1 TAR RNA element form RNA/DNA kissing complexes. *J. Biol. Chem.* **274**: 12730-12737.

Brunel C, Marquet R, Romby P, Ehresmann C. 2002. RNA loop-loop interactions as dynamic functional motifs. *Biochimie* **84**: 925-44.

Chang KY, Tinoco I, Jr. 1994. Characterization of a "kissing" hairpin complex derived from the human immunodeficiency virus genome. *Proc Natl Acad Sci U S A* **91**: 8705-9.

Chang KY, Tinoco I, Jr. 1997. The structure of an RNA "kissing" hairpin complex of the HIV TAR hairpin loop and its complement. *J Mol Biol* **269**: 52-66.

Christ D, Winter G. 2003. Identification of functional similarities between proteins using directed evolution. *Proc Natl Acad Sci U S A* **100**: 13202-6.

Collin D, Heijenoort C, Boiziau C, Toulmé JJ, Guittet E. 2000. NMR characterization of a kissing complex formed between the TAR RNA element of HIV-1 and a DNA aptamer. *Nucleic Acids Res* **28**: 3386-3391.

Comolli LR, Pelton JG, Tinoco I, Jr. 1998. Mapping of a protein-RNA kissing hairpin interface: Rom and Tar-Tar*. *Nucleic Acids Res* **26**: 4688-95.

Darfeuille F, Cazenave C, Gryaznov S, Ducongé F, Di Primo C, Toulmé JJ. 2001. RNA and N3'-->P5' kissing aptamers targeted to the trans-activation responsive (TAR) RNA of the human immunodeficiency virus-1. *Nucleosides Nucleotides Nucleic Acids* **20**: 441-9.

Darfeuille F, Reigadas S, Hansen JB, Orum H, Di Primo C, Toulmé JJ. 2006. Aptamers targeted to an RNA hairpin show improved specificity compared to that of complementary oligonucleotides. *Biochemistry* **45**: 12076-82.

Di Primo C, Lebars I. 2007. Determination of refractive index increment ratios for protein-nucleic acid complexes by surface plasmon resonance. *Anal Biochem* **368**: 148-55.

Ducongé F, Di Primo C, Toulmé JJ. 2000. Is a closing "GA pair" a rule for stable loop-loop RNA complexes? *J Biol Chem* **275**: 21287-94.

Ducongé F, Toulmé JJ. 1999. In vitro selection identifies key determinants for loop-loop interactions: RNA aptamers selective for the TAR RNA element of HIV-1. *RNA* **5**: 1605-14.

Eberle W, Pastore A, Sander C, Rosch P. 1991. The structure of ColE1 rop in solution. *J Biomol NMR* **1**: 71-82.

Eguchi Y, Tomizawa J. 1990. Complex formed by complementary RNA stem-loops and its stabilization by a protein: function of CoIE1 Rom protein. *Cell* **60**: 199-209.

Eguchi Y, Tomizawa J. 1991. Complexes formed by complementary RNA stem-loops. Their formations, structures and interaction with ColE1 Rom protein. *J Mol Biol* **220**: 831-42.

Ennifar E, Walter P, Ehresmann B, Ehresmann C, Dumas P. 2001. Crystal structures of coaxially stacked kissing complexes of the HIV-1 RNA dimerization initiation site. *Nat Struct Biol* **8**: 1064-8.

Fisher RJ, Fivash MJ, Stephen AG, Hagan NA, Shenoy SR, Medaglia MV, Smith LR, Worthy KM, Simpson JT, Shoemaker R, McNitt KL, Johnson DG, Hixson CV, Gorelick RJ, Fabris D, Henderson LE, Rein A. 2006. Complex interactions of HIV-1 nucleocapsid protein with oligonucleotides. *Nucleic Acids Res* **34**: 472-84.

Fivash M, Towler EM, Fisher RJ. 1998. BIAcore for macromolecular interaction. *Curr Opin Biotechnol* **9**: 97-101.

Geisinger E, Adhikari RP, Jin R, Ross HF, Novick RP. 2006. Inhibition of rot translation by RNAIII, a key feature of agr function. *Mol Microbiol* **61**: 1038-48.

Gregorian RS, Jr., Crothers DM. 1995. Determinants of RNA hairpin loop-loop complex stability. *J Mol Biol* **248**: 968-84.

Jang SB, Jeong MS, Carter RJ, Holbrook EL, Comolli LR, Holbrook SR. 2006. Novel crystal form of the ColE1 Rom protein. *Acta Crystallogr D Biol Crystallogr* **62**: 619-27.

Joss L, Morton TA, Doyle ML, Myszka DG. 1998. Interpreting kinetic rate constants from optical biosensor data recorded on a decaying surface. *Anal Biochem* **261**: 203-10.

Karlsson R, Katsamba PS, Nordin H, Pol E, Myszka DG. 2006. Analyzing a kinetic titration series using affinity biosensors. *Anal Biochem* **349**: 136-47.

Karlsson R, Roos H, Fagerstam L, Persson B. 1994. Kinetic and concentration analysis using BIA technology. *Methods* **1994**: 99-110.

Kim CH, Tinoco I, Jr. 2000. A retroviral RNA kissing complex containing only two G.C base pairs. *Proc Natl Acad Sci U S A* **97**: 9396-401.

Law MJ, Rice AJ, Lin P, Laird-Offringa IA. 2006. The role of RNA structure in the interaction of U1A protein with U1 hairpin II RNA. *Rna* **12**: 1168-78.

Lee AJ, Crothers DM. 1998. The solution structure of an RNA loop-loop complex: the ColE1 inverted loop sequence. *Structure* **6**: 993-1005.

Li PT, Bustamante C, Tinoco I, Jr. 2006. Unusual mechanical stability of a minimal RNA kissing complex. *Proc Natl Acad Sci U S A* **103**: 15847-52.

Morton TA, Myszka DG. 1998. Kinetic analysis of macromolecular interactions using surface plasmon resonance biosensors. *Methods Enzymol* **295**: 268-94.

Muriaux D, Fosse P, Paoletti J. 1996. A kissing complex together with a stable dimer is involved in the HIV-1Lai RNA dimerization process in vitro. *Biochemistry* **35**: 5075-82.

Myszka DG. 1999. Improving biosensor analysis. *J Mol Recognit* **12**: 279-84.

Paillart JC, Skripkin E, Ehresmann B, Ehresmann C, Marquet R. 1996. A loop-loop "kissing" complex is the essential part of the dimer linkage of genomic HIV-1 RNA. *Proc Natl Acad Sci USA* **93**: 5572-5577.

Paillart JC, Westhof E, Ehresmann C, Ehresmann B, Marquet R. 1997. Non-canonical interactions in a kissing loop complex: the dimerization initiation site of HIV-1 genomic RNA. *J Mol Biol* **270**: 36-49.

Predki PF, Nayak LM, Gottlieb MB, Regan L. 1995. Dissecting RNA-protein interactions: RNA-RNA recognition by Rop. *Cell* **80**: 41-50.

Rich RL, Myszka DG. 2006. Survey of the year 2005 commercial optical biosensor literature. *J Mol Recognit* **19**: 478-534.

Rist M, Marino J. 2001. Association of an RNA kissing complex analyzed using 2-aminopurine fluorescence. *Nucleic Acids Res* **29**: 2401-8.

Sjölander S, Urbaniczky C. 1991. Integrated fluid handling system for biomolecular interaction analysis. *Anal Chem* **63**: 2338-45.

Song Y, Friebe P, Tzima E, Junemann C, Bartenschlager R, Niepmann M. 2006. The hepatitis C virus RNA 3'-untranslated region strongly enhances translation directed by the internal ribosome entry site. *J Virol* **80**: 11579-88.

Tumolo T, Angnes L, Baptista MS. 2004. Determination of the refractive index increment (dn/dc) of molecule and macromolecule solutions by surface plasmon resonance. *Anal Biochem* **333**: 273-279.

Van Regenmortel MH. 2001. Analysing structure-function relationships with biosensors. *Cell Mol Life Sci* **58**: 794-800.